HNUE JOURNAL OF SCIENCE DOI: 10.18173/2354-1059.2023-0024
Natural Sciences 2023, Volume 68, Issue 2, pp. 97-111
This paper is available online at http://stdb.hnue.edu.vn

THE ADSORPTION OF TOXIC GAS MOLECULES (CO, CO_2, NO_2) ON SILICENE, GERMANENE AND STANENE: A FIRST-PRINCIPLES STUDY

Pham Duy Thanh[1] and Tran Phan Thuy Linh[2]
[1]*High School for Gifted Students, Hanoi National University of Education*
[2]*Faculty of Physics, Hanoi National University of Education*

Abstract. The adsorption of toxic gas molecules on Xenes (X = Si, Ge, Sn) has been studied by density functional theory (DFT). The optimized adsorption site of the adsorbates (CO, CO_2, NO_2) on Xenes (X = Si, Ge, Sn), the corresponding adsorption energies, band gap, band structure, and density of states of silicene, germanene, and stanene are discussed. We observed that Xenes (X = Si, Ge, Sn) weakly physically adsorb CO and CO_2 with adsorption energies not larger than 0.201 eV, from which we show that Xenes (X = Si, Ge, Sn) are not suitable for gas sensing application of CO and CO_2. On the other hand, NO_2 can be adsorbed on Xenes (X = Si, Ge, Sn) with moderate adsorption energy (respectively 0.813 eV, 0.716 eV, and 0.776 eV). In addition, the band gap of Xenes (X = Si, Ge, Sn) is expanded after adsorption of NO_2 in varying degrees, which indicates that Xenes (X = Si, Ge, Sn) may be a promising candidate as the sensor of NO_2. Finally, we assume that Xenes (X = Si, Ge, Sn) has no potential in developing catalysts for CO, CO_2, and NO_2 due to these gas molecules are not strongly chemisorbed on Xenes (X = Si, Ge, Sn) (adsorption energies < 1.00 eV). Our research results not only help to understand the properties of Xenes (X = Si, Ge, Sn) but also suggest research directions for the application of its potential as catalysts and gas sensors as well as applications in the electronics industry.

Keywords: DFT, silicene, germanene, stanene, adsorption.

1. Introduction

Over 80 years ago, when the debate over the existence of two-dimensional (2D) materials was discussed in the theoretical physics community worldwide, Peierls and Landau presented an argumentative paper stating that 2D materials are thermodynamically unstable and therefore cannot exist in the natural world [1, 2]. Their theory revealed that thermal fluctuations in low-dimensional crystal lattices would cause atomic displacements comparable to the interatomic distances at any temperature, leading to the disruption of the two-dimensional crystal lattice structure [3]. Later, in 1968,

Received June 5, 2023. Revised June 24, 2023. Accepted June 30, 2023.
Contact Pham Duy Thanh, e-mail address: pdthanh@hnue.edu.vn

Mermin published the results of his experiments, all of which demonstrated that the melting temperature of thin films decreased rapidly as their thickness decreased, and the films became unstable. At a thickness of a few tens of atomic layers, the films either disintegrated or clustered together to form three-dimensional structures [4]. Mermin's experimental findings contributed to reinforcing the arguments made by Peierls and Landau. However, many scientists did not give up their research on 2D materials due to their numerous advantageous theoretical properties.

In 2004, a group of scientists led by Novoselov and Geim successfully synthesized the world's first 2D material called graphene [5]. It is a single-layer sheet of graphite (carbon) with a thickness of only a few atoms, yet it remains stable under ambient conditions [5]. When electric currents pass through graphene, the charge carriers were observed to have an exceptionally large mean free path or mobility, with particle speeds reaching about three percent of the speed of light [5]. Furthermore, graphene exhibits extremely high thermal conductivity [6], nearly perfect optical transparency [7, 8], and its mechanical strength surpasses that of diamond [5]. These outstanding properties demonstrate the tremendous potential of graphene for various emerging technologies.

Research on 2D materials has experienced significant growth since the remarkable properties of graphene were experimentally confirmed. In the short period following that, a plethora of papers on 2D materials has been published. One of the research directions that has garnered attention from theoretical physicists is the gas adsorption capability of 2D materials, particularly for toxic gases that can contribute to environmental pollution and pose health risks to humans. The investigation of gas adsorption ability aims to develop high-sensitivity sensors for detecting hazardous gases. The gas adsorption capacity of each 2D material varies depending on the specific gas. Previous studies have shown that graphene only weakly physically adsorbs the gas molecule NO, making it unsuitable for detecting this particular gas [9]. However, silicene exhibits a moderate adsorption capability for NO gas with an adsorption energy of 0.35 eV, making it a potential candidate for NO gas sensors [10]. Therefore, the selection of suitable 2D materials for sensor applications depends on factors such as commercial viability and gas adsorption capabilities specific to each gas type. Continuing in that research direction, the gas adsorption capacities of free-standing silicene, germanene, and stanene towards some common toxic gases (CO, CO_2, NO_2) are being investigated. These gases are often produced during the combustion of coal, oil, natural gas, etc., and can be present in everyday kitchen environments. Silicene, germanene, and stanene are collectively known as Xenes, which are defined as monolayer materials with an element and with a similar structure to graphene. The calculations are performed using the CASTEP code available in the Materials Studio software, based on density functional theory (DFT).

2. Content

2.1. Computational methods and models

The DFT calculations were performed using the CASTEP code available in the Materials Studio (MS) software. The exchange-correlation energy function used was the Perdew-Burke-Ernzerhof (PBE) approximation within the generalized gradient

approximation (GGA). The supercell of Xenes was chosen to be 3×3, containing 18 atoms. Along the perpendicular direction to the Xenes surface, the height of the supercell was set to be 30 to avoid the interactions between periodic images. Silicene, germanene, and stanene have a honeycomb-like structure similar to graphene, but their crystal lattice is not flat like graphene. Instead, they have a buckled structure (Figure 1). The theoretical calculations using DFT revealed that the optimized structure of silicene has a Si-Si bond length of a = 2.270 Å, and a buckling height between the two sublattices A and B of h = 0.46 Å, with sublattice A having smaller z-coordinate values (Figure 1). On the other hand, the corresponding values for germanene are a = 2.394 Å and h = 0.69 Å, and for stanene, a = 2.746 Å and h = 0.81 Å [11].

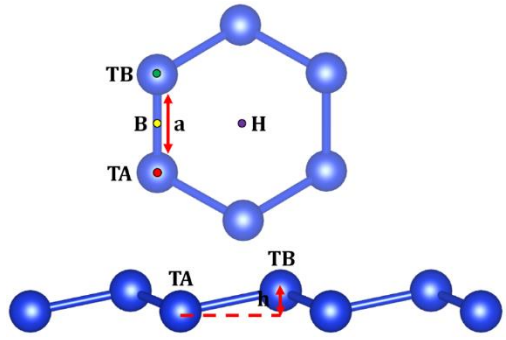

Figure 1. The buckled hexagonal structure of silicene, the four adsorption sites considered H, TA, TB, and B, and the sublattices A and B.

In DFT calculations, most of the calculations are integrals of the form

$$\bar{f} = \frac{1}{V_{\mathrm{BZ}}} \int_{\mathrm{BZ}} f(\mathbf{k}) d\mathbf{k}, \tag{1}$$

where V_{BZ} is the volume of the Brillouin zone and $f(\mathbf{k})$ is a periodic function of the wave vector $\mathbf{k}$ with period given by reciprocal lattice vector $\mathbf{G}$. This integral is defined in reciprocal space and regions of the integral are the possible values of $\mathbf{k}$ in the Brillouin zone.

The integral in equation (1) is calculated approximately by the special-point technique [12]

$$\bar{f} = \sum_{i=1}^{N_{\mathbf{k}}} \omega_i f(\mathbf{k}_i), \tag{2}$$

where $N_{\mathbf{k}}$ is a set of points such that

$$\frac{1}{V_{\mathrm{BZ}}} \int_{\mathrm{BZ}} d\mathbf{k} = \sum_{i=1}^{N_{\mathbf{k}}} \omega_i = 1 \tag{3}$$

and the value of the sum in equation (2) converges to the exact value of the integral in equation (1). Most of the current packages for DFT calculation use the method of choosing k-points, which was researched and developed by Monkhorst and Pack in 1976 [13]. In this proposed method, the number of special points is determined for each direction in reciprocal space. In our study, we chose the Monkhorst-Pack k-points grid of 3×3×1 to sample the Brillouin zone with 13 special points and with 3 inequivalent points in the irreducible Brillouin zone. The convergence criteria were met when the atomic force acting on each atom was below 0.025 eV/Å and the energy threshold was below 10 eV.

Theoretically, the wave function ψ_k of an electron in a periodic lattice is a linear combination of an infinite of basis wave functions

$$\psi_k = \sum_{\mathbf{G}} C_{\mathbf{G}} e^{i(\mathbf{k}+\mathbf{G}).\mathbf{r}}, \quad (4)$$

each basis wave function corresponds to a possible value of the reciprocal lattice vector *G*. In actual calculations, the number of basis wave functions must be finite, so the linear combination of the chosen basis wave functions is approximately ψ_k. Thefore, the possible value of **G** is limited to less than a cutoff value

$$G_{\text{cut}} = \frac{\sqrt{2m_e E_{\text{cut}}}}{\hbar}, \quad (5)$$

where E_{cut} is called energy cutoff. Choosing the suitable value of Ecut (or Gcut) is the first task for any DFT calculations because it affects the accuracy of results then, moreover, it reduces computing resources because of unnecessary calculations when the result reached convergence. Therefore, the suitable value of E_{cut} is the value at which the total energy of the system begins to converge. To investigate the convergence of the total energy for each adsorbent material when CO gas molecules are adsorbed on the surface, we performed calculations at different energy cutoff values (E_{cut}) for the plane wave basis set. The CO gas molecule was adsorbed at the TB site with the C–X distance set to d = 3.00 Å and the X-O-C angle set to 180° (X = Si, Ge, Sn). Energy cutoff was varied in the range of 400 eV to 850 eV.

Table 1 shows the results for the total energy of the CO/Xenes system and the corresponding calculation time. Figure 2 shows that the convergence begins to occur with E_{cut} = 700 eV. Figure 3 shows that the computation time increases if the value of E_{cut} is increased respectively, even after the results have achieved convergence. This result is consistent with both CO_2/Xenes and NO_2/Xenes systems. Therefore, the energy cutoff value of E_{cut} = 700 eV is chosen for all remaining calculations.

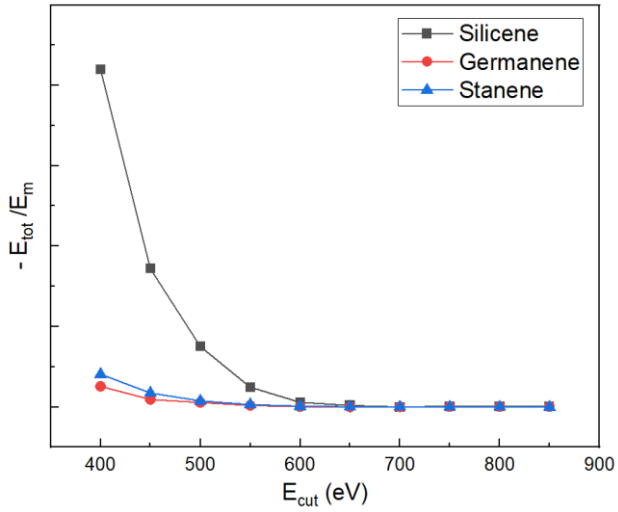

Figure 2. The convergence of the total energy according to the energy cutoff

Table 1. Total energy (E_{tot}) of the molecule-Xenes system (E_{tot}) and calculate time (T_{cal}) according to energy cutoff (E_{cut})

Adsorbent	E_{cut} **(eV)**	E_{tot} **(eV)**	T_{cal} **(s)**
Silicene	400	−3651.28262	1583.88
	450	−3652.18742	1792.42
	500	−3652.54075	3152.53
	550	−3652.72566	4603.12
	600	−3652.79446	4922.27
	650	−3652.80851	5471.09
	700	−3652.81528	5884.73
	750	−3652.81185	6553.28
	800	−3652.81230	6848.77
	850	−3652.81375	7543.53
Germanene	400	−46276.8462	3583.56
	450	−46277.6030	4659.70
	500	−46277.7723	5619.34
	550	−46277.9487	6286.22
	600	−46278.0186	6286.22
	650	−46278.0315	7938.48
	700	−46278.0232	9117.23
	750	−46278.0178	10317.72
	800	−46278.0163	11664.00
	850	−46278.0175	12501.30
Stanene	400	−37672.9316	5014.30
	450	−37673.8105	5698.78
	500	−37674.1770	6755.67
	550	−37674.3544	7934.14
	600	−37674.4301	9604.89
	650	−37674.4528	10447.09
	700	−37674.4591	14230.41
	750	−37674.4590	14596.81
	800	−37674.4615	14708.50
	850	−37674.4638	15530.52

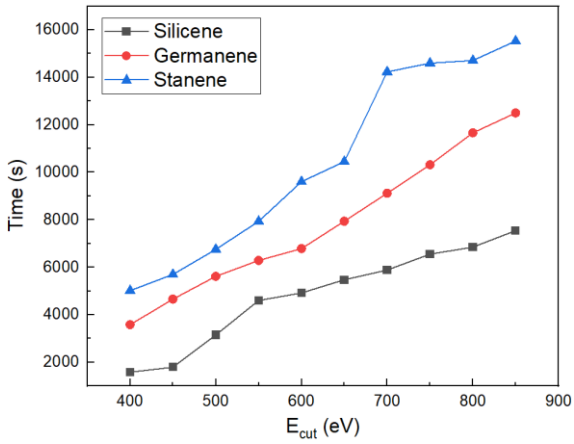

Figure 3. Calculate time according to energy cutoff

First, we use this computational model to consider pristine Xenes (X = Si, Ge, Sn) to calculate band structure. It can be seen from Figure 4 that silicene is a semiconductor with a zero band gap, the π, and π* band intersecting linearly at the Fermi level to form a "Dirac cone" at the K symmetry point in the reciprocal space. This result is in good agreement with the previous results [14-16], which shows the suitability of the adopted methods in the present work is enough to calculate in the following section.

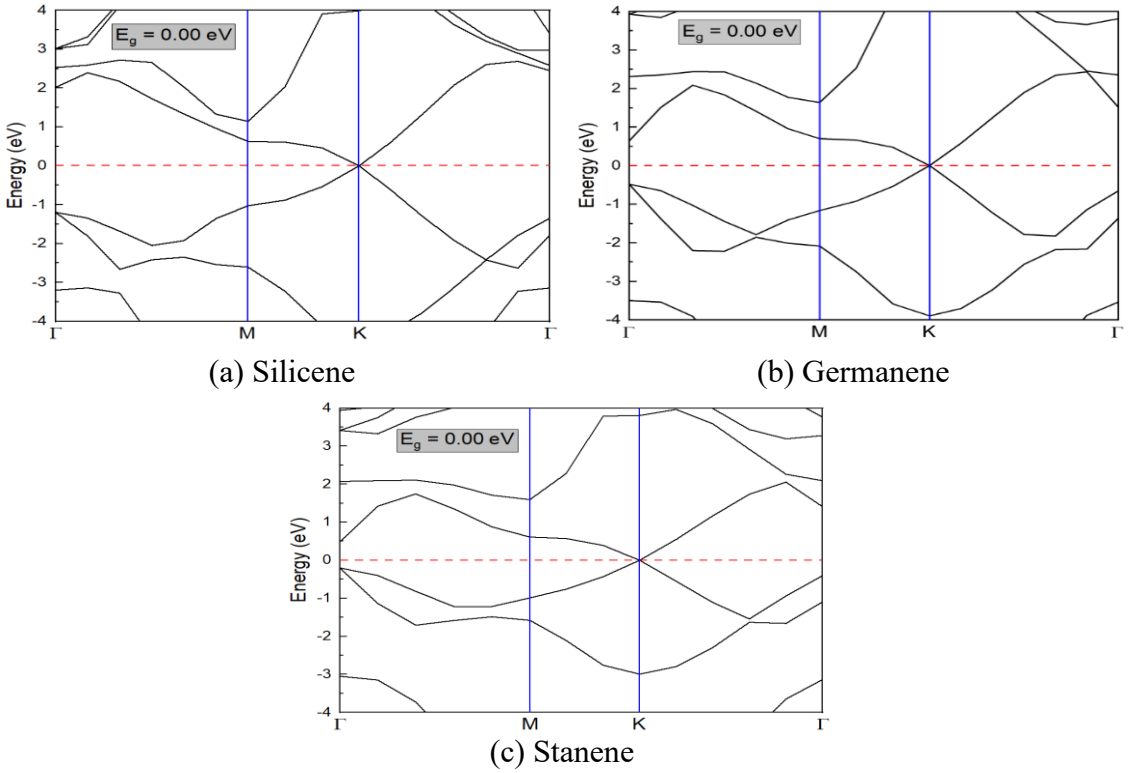

(a) Silicene (b) Germanene

(c) Stanene

Figure 4. Band structure of pristine Xenes

2.2. The optimized adsorption site

For each adsorbing molecule, four adsorption sites are investigated: on top of the hexagon center (H - Hollow), on top of the bond center (B - Bridge), on top of each atom in sublattice A (TA - Top A), and on top of each atom in sublattice B (TB - Top B) (refer to Figure 1). For the optimal adsorption position, different orientations of the adsorbing molecule are also explored for optimization. The total energy of each adsorbing molecule at the B, H, TA, and TB positions (refer to Figure 1) is examined, with a fixed distance between the adsorbates (CO, CO_2, NO_2) and the surface of Xenes (X = Si, Ge, Sn) at d = 3.00 Å. The data are recorded in Table 2.

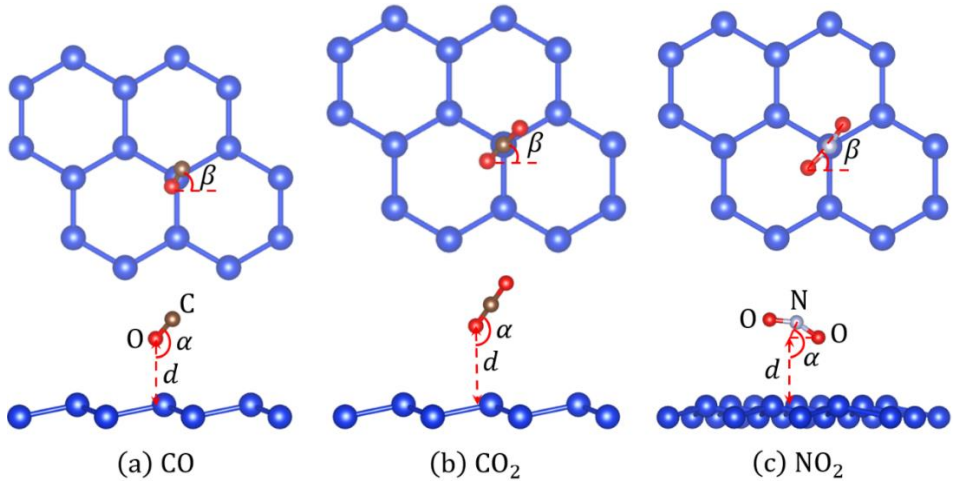

Figure 5. Molecules on silicene surface

Table 2. Total energy (Etot) of the molecule-Xenes system for various adsorption sites of the molecule

Adsorbate	**Site**	***α***	***β***	E_{tot} **(eV)**		
				Silicene	***Germanene***	***Stanene***
CO	TA	180°	-	−3652.85414	−46278.0820	−37674.5720
	TB	180°	-	−3652.88789	−46278.1208	−37674.5513
	TB	0°	-	−3652.91620	−46278.1379	−37674.6217
	TB	90°	0°	−3652.85107	−46278.0888	−37674.5713
	TB	90°	90°	−3652.85448	−46278.1011	−37674.5720
	TB	10°	90°	**−3652.92650**	**−46278.1399**	**−37674.6220**
	TB	20°	90°	−3652.92491	−46278.1387	−37674.6202
	TB	30°	90°	−3652.92253	−46278.1366	−37674.6171
	TB	40°	90°	−3652.91822	−46278.1324	−37674.6124
	TB	50°	90°	−3652.91110	−46278.1264	−37674.6057
	TB	60°	90°	−3652.90082	−46278.1182	−37674.5967

	TB	70°	90°	−3652.88647	−46278.1070	−37674.5856
	TB	80°	90°	−3652.86658	−46278.0911	−37674.5709
	B	180°	-	−3652.84041	−46278.0620	−37674.4591
	H	180°	-	−3652.81528	−46278.0315	−37674.5713
CO_2	TA	180°	-	−4094.23711	−46719.4564	−38115.9343
	TB	180°	-	−4094.25945	−46719.4765	−38115.9615
	TB	90°	0°	−4094.17953	−46719.4110	−38115.9094
	TB	90°	90°	−4094.18264	−46719.4166	−38115.9125
	TB	100°	90°	−4094.26319	−46719.4628	−38115.9422
	TB	110°	90°	−4094.27653	−46719.4823	−38115.9678
	TB	120°	90°	**−4094.27741**	**−46719.4848**	**−38115.9719**
	TB	130°	90°	−4094.27551	−46719.4829	−38115.9700
	TB	140°	90°	−4094.27392	−46719.4807	−38115.9608
	TB	150°	90°	−4094.27320	−46719.4794	−38115.9658
	TB	160°	90°	−4094.27292	−46719.4788	−38115.9651
	TB	170°	90°	−4094.27291	−46719.4784	−38115.9650
	B	180°	-	−4094.23349	−46719.4462	−38115.9206
	H	180°	-	−4094.21165	−46719.4205	−38115.8749
NO_2	TA	180°	0°	−4209.28961	−46834.5790	−38231.0991
	TB	180°	0°	−4209.35691	−46834.6120	−38231.2510
	TB	180°	90°	−4209.35709	−46834.6121	−38231.2511
	TB	0°	0°	−4209.45302	−46834.6928	−38231.3215
	TB	0°	90°	**−4209.45359**	**−46834.6929**	**−38231.3218**
	TB	10°	90°	−4209.45269	−46834.6920	−38231.3201
	TB	20°	90°	−4209.45142	−46834.6908	−38231.3171
	TB	30°	90°	−4209.44853	−46834.6891	−38231.3142
	B	180°	0°	−4209.32543	−46834.5320	−38231.1986
	H	180°	0°	−4209.28644	−46834.5311	−38231.0897

When adsorbing gas molecules onto the surface of Xenes (X = Si, Ge, Sn), the most favorable adsorption position is the one with the strongest bond, which corresponds to the lowest total energy of the system. From Table 2, it can be observed that the most stable configuration of CO on Xenes (X = Si, Ge, Sn) occurs when the carbon atom is bonded to the TB position of Xenes (X = Si, Ge, Sn) with the X-C-O angle approximately equal to 170°. For CO_2, the optimal adsorption position on the surface of Xenes (X = Si, Ge, Sn) is the TB position with the X-O-C angle (X = Si, Ge, Sn) being 120°. In the most stable

configuration of NO_2 on Xenes (X = Si, Ge, Sn), the nitrogen atom of the NO_2 molecule bonds to the X atom (X = Si, Ge, Sn) in the TB position, with both oxygen atoms having the same distance to the Xenes surface. The calculated results also indicate that the adsorption positions and optimal orientations of the three gas molecules CO, CO_2, and NO_2 on Xenes (X = Si, Ge, Sn) are the same, which could be attributed to the similar characteristics of these three types of 2D materials.

2.3. Binding distance and adsorption energy

After determining the optimal adsorption positions of the gas molecules on the surface of Xenes (X = Si, Ge, Sn), we investigated the binding distance (*d*) that corresponds to the strongest bond, i.e., the highest adsorption energy. The adsorption energy (E_{ad}) of the gas molecules on the Xenes surface is defined as follows:

$$E_{ad} = E_{molecule} + E_{Xenes} - E_{molecule/Xenes},$$

where $E_{molecule}$, $E_{Xenes,}$ and $E_{molecule/Xenes}$ represent the energy of the isolated gas molecule, the energy of an Xenes supercell, and the interaction energy (or total energy) of the gas molecule and Xenes system, respectively. With this definition, a larger value of Ead indicates stronger adsorption of the gas molecules on Xenes. Additionally, the positive adsorption energy corresponds to an exothermic process, where heat is released. In such cases, spontaneous changes in physical and chemical properties can occur without external influence.

Table 3. Binding distance (d) and adsorption energy (E_{ad}) for the optimized adsorption site of various adsorbates on Xenes

Adsorbate	***d* (Å)**		**E_{ad} (eV)**	
		Silicene	***Germanene***	***Stanene***
CO	2.20	0.044	0.100	0.140
	2.40	0.098	0.138	0.166
	2.60	0.134	0.164	0.181
	2.80	0.157	0.179	0.189
	3.00	0.171	0.198	0.193
	3.20	0.177	**0.201**	**0.194**
	3.40	0.179	0.190	0.192
	3.60	**0.180**	0.188	0.189
	3.80	0.178	0.186	0.187
	4.00	0.176	0.183	0.184
	4.20	0.174	0.180	0.181
	4.40	0.171	0.178	0.179
	4.60	0.169	0.175	0.176
	4.80	0.167	0.173	0.174
	5.00	0.165	0.161	0.172

CO_2	3.20	0.015	0.025	0.023
	3.40	0.020	**0.028**	**0.025**
	3.60	**0.021**	0.027	0.024
	3.80	0.020	0.025	0.022
	4.00	0.019	0.023	0.021
	4.20	0.016	0.021	0.018
	4.40	0.014	0.019	0.016
	4.60	0.013	0.017	0.015
	4.80	0.011	0.015	0.012
NO_2	1.90	0.689	0.335	-
	2.20	0.787	0.560	0.119
	2.10	**0.813**	0.673	0.455
	2.20	0.796	**0.716**	0.646
	2.30	0.754	0.715	0.742
	2.40	0.700	0.688	**0.776**
	2.50	0.640	0.648	0.772
	2.60	0.578	0.598	0.744
	2.70	0.519	0.546	0.701
	2.80	0.464	0.495	0.652
	2.90	0.464	0.448	0.600
	3.00	0.368	0.406	0.548

The adsorption energy of a foreign species on an adsorbent is an important criterion for evaluating its chemical reactivity. Therefore, we have calculated the adsorption energies and presented them in Table 3. From Table 3, it can be observed that CO and CO_2 are weakly physisorbed on Xenes (X = Si, Ge, Sn) with relatively large binding distance (> 3.20 Å) and small adsorption energy. Specifically, for silicene, the adsorption energies are 0.180 eV and 0.021 eV for CO and CO_2, respectively. For germanene, the values are 0.201 eV and 0.028 eV, and for stanene, they are 0.194 eV and 0.025 eV. On the other hand, NO_2 can be chemically adsorbed on Xenes (X = Si, Ge, Sn) with moderate adsorption energies of 0.813 eV, 0.716 eV, and 0.776 eV, respectively. Therefore, Xenes (X = Si, Ge, Sn) can be utilized as a sensor for detecting NO_2 due to the easily established adsorption-desorption equilibrium of NO_2 on Xenes (X = Si, Ge, Sn). None of the gases in the three categories mentioned exhibit strong reactivity with Xenes (X = Si, Ge, Sn) (adsorption energies < 1.00 eV), indicating that Xenes (X = Si, Ge, Sn) are unsuitable as a catalyst for CO, CO_2, and NO_2.

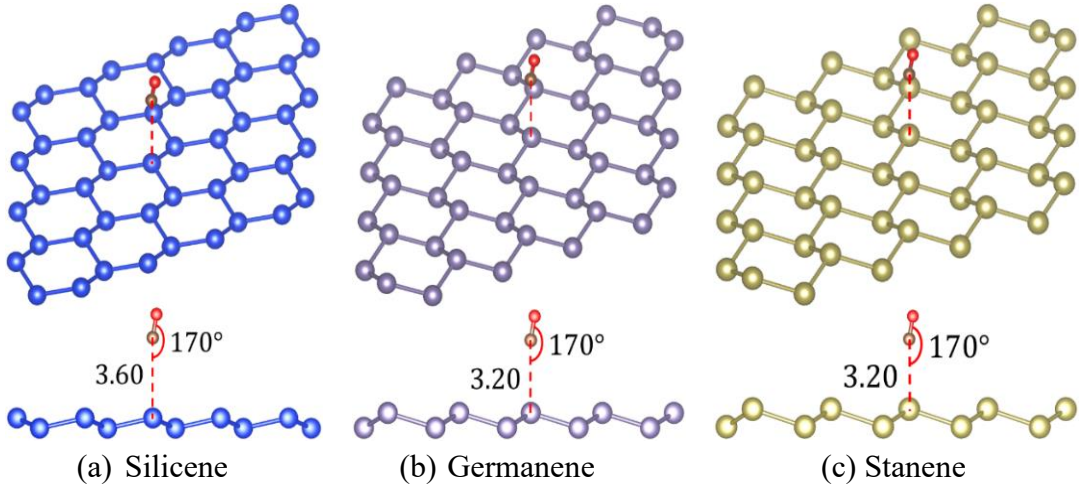

Figure 6. The most stable configuration for CO on Xenes

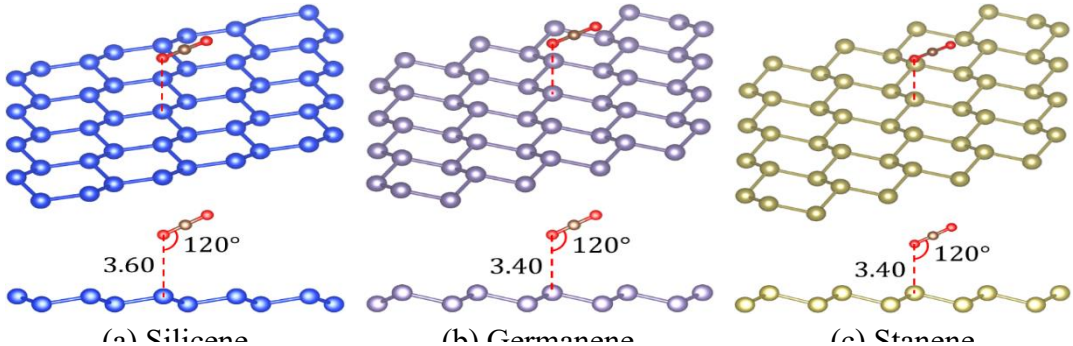

Figure 7. The most stable configuration for CO_2 on Xenes

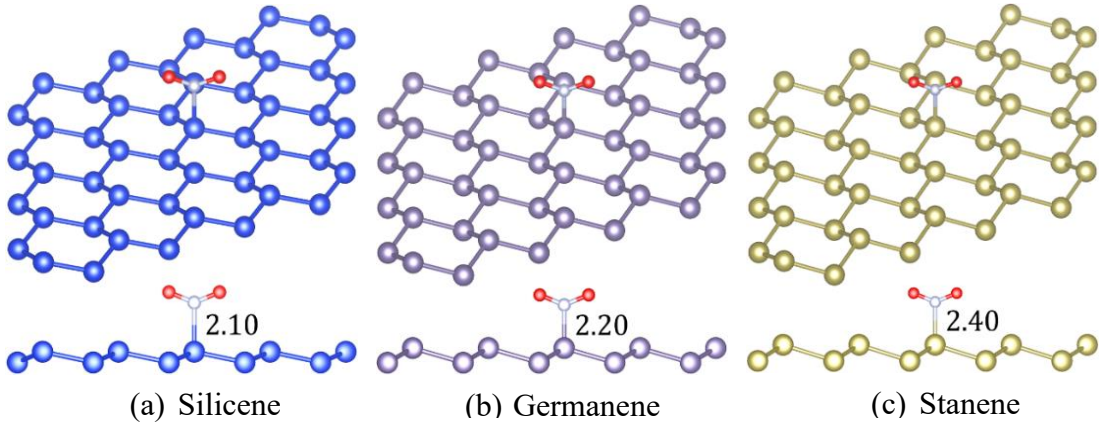

Figure 8. The most stable configuration for NO_2 on Xenes

2.4. Band gap, band structure, and density of states

The change in the band gap width upon the adsorption of gas molecules can lead to a variation in the electrical conductivity of the adsorbent material, which can be applied in gas sensing applications. Therefore, we have calculated the band gap width and presented it in Table 4.

Table 4. Adsorption energy (E_{ad}) and band gap width (E_g) of Xenes for the most stable configuration

Adsorbate	*d* (Å)	E_{ad} (eV)	E_g (eV)
Silicene			
CO	3.40	0.180	~0.00
CO_2	3.60	0.021	~0.00
NO_2	2.10	0.813	0.042
Germanene			
CO	3.20	0.201	~0.00
CO_2	3.40	0.028	~0.00
NO_2	2.20	0.716	0.024
Stanene			
CO	3.20	0.194	~0.00
CO_2	3.40	0.025	~0.00
NO_2	2.40	0.776	0.015

From Table 4, it can be observed that Xenes (X = Si, Ge, Sn) are suitable for use as gas sensors for NO_2, with silicene being more suitable than germanene and stanene due to more pronounced changes in the band gap width. On the other hand, the weak physisorption of CO and CO_2 molecules hardly alters the band gap of Xenes (X = Si, Ge, Sn), indicating their low (or no) sensitivity to these gases.

To better understand the changes in the electronic properties of Xenes (X = Si, Ge, Sn) induced by NO_2 adsorption, the energy band structure and density of states (DOS) of Xenes (X = Si, Ge, Sn) after NO_2 adsorption have been calculated and presented in Figure 9 (with the Fermi level set at 0). Although the DFT-PBE method underestimates the band gap, it still provides reasonable features of the electronic structure. Comparing Figure 9 with the band structures of pristine Xenes (X = Si, Ge, Sn) (Figure 4), it can be observed that NO_2 adsorption expands the band gap of Xenes (X = Si, Ge, Sn) to varying degrees, transforming them from zero band gap semiconductors to narrow gap semiconductors.

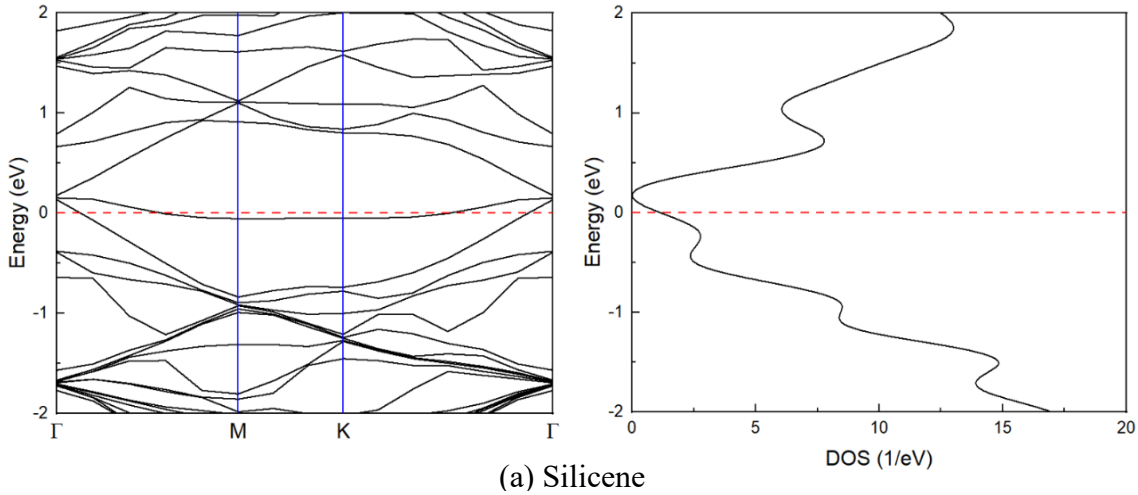

(a) Silicene

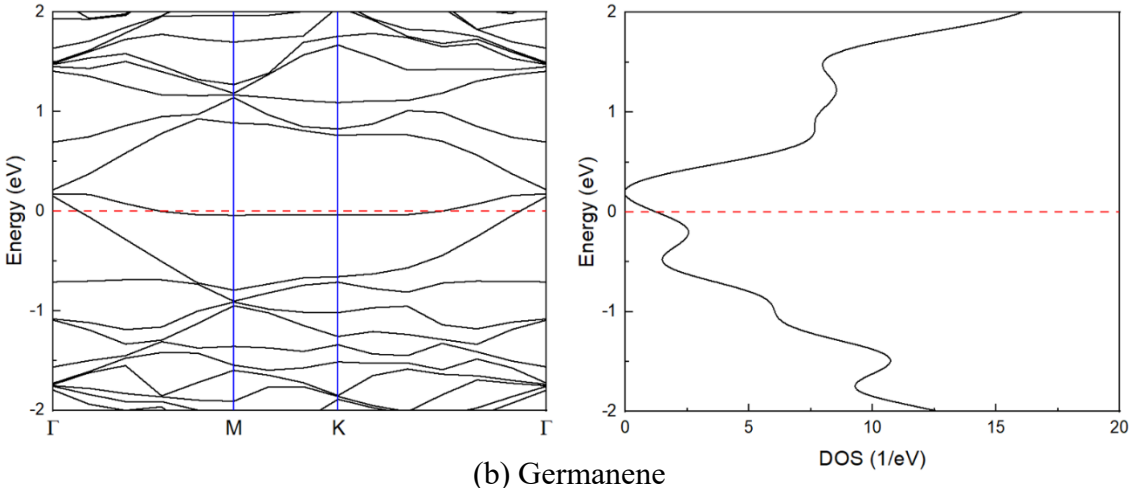

(b) Germanene

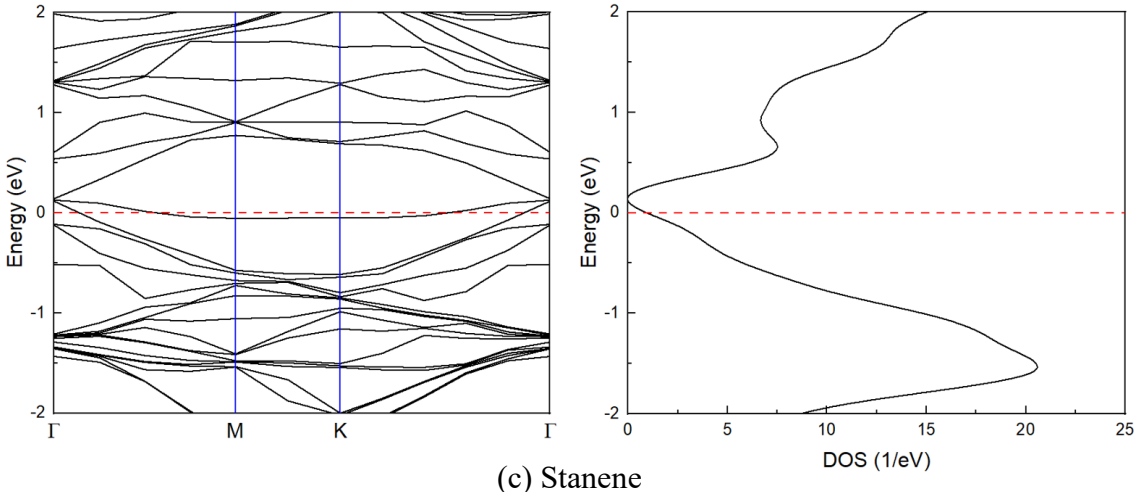

(c) Stanene

Figure 9. Band structure, density of states (DOS) of Xenes after NO_2 adsorption

3. Conclusions

In conclusion, we have utilized DFT to conduct a research study evaluating the optimized adsorption positions and adsorption mechanisms (adsorption energy, binding distance) of certain gas molecules (CO, CO_2, NO_2) on 3×3 silicene, germanene, and stanene. The results indicate that: (1) CO, CO_2, and NO_2 molecules are adsorbed on Xenes (X = Si, Ge, Sn) surface in the TB site with the inclination angle of each gas molecule on all three adsorbents being the same. The most stable configuration for NO_2 on Xenes is that its N atom binds with the TB site of Xenes with the X-Si (X = Si, Ge, Sn) distance of 2.10 Å, 2.20 Å, and 2.40 Å, respectively, which is smaller than the X-C bond (X = Si, Ge, Sn) about 1.00 Å to 1.50 Å in the case of CO and CO_2 adsorption; (2) Xenes (X = Si, Ge, Sn) do not exhibit potential as catalysts for CO, CO_2, and NO_2; (3) Xenes (X = Si, Ge, Sn) are not suitable as the sensor of CO and CO_2; (4) NO_2 can be chemically adsorbed on Xenes (X = Si, Ge, Sn) with moderate adsorption energy, accompanied by band gap expansion. Therefore, Xenes (X = Si, Ge, Sn) can be promising candidates for NO_2 gas sensors.

Possible future research directions could include: (1) Improving calculations by increasing the size of the unit cell of Xenes to neglect the interactions between adsorbed molecules, which would require significantly more computational resources due to the increased number of atoms in a larger supercell; (2) Further investigating the essential characteristics of gas sensors such as the stability, work function, selectivity, sensitivity and recovery time of Xenes (X = Si, Ge, Sn) in the sensing process.

REFERENCES

[1] Rudolf Peierls**,** 1935. Quelques proprietes typiques des corps solides. *Annales de l'institut Henri Poincare,* Vol. 05, pp. 177-222.

[2] Lev Davidovich Landau, 1937. Zur theorie der phasenumwandlungen ii. *Phys. Z. Sowjetunion,* Vol. 11, Iss. 545, pp. 26-35.

[3] LD Landau and EM Lifshitz, 1980. *Statistical physics, part i.* Pergamon press, Oxford.

[4] N David Mermin, 1968. Crystalline order in two dimensions. *Physical Review*, Vol. 176, Iss. 1, pp 250.

[5] Kostya S Novoselov, Andre K Geim, Sergei V Morozov, De-eng Jiang, Yanshui Zhang, Sergey V Dubonos, Irina V Grigorieva, and Alexandr A Firsov, 2004. Electric field effect in atomically thin carbon films. *Science,* Vol. 306, Iss. 5696, pp. 666-669.

[6] Alexander A Balandin, Suchismita Ghosh, Wenzhong Bao, Irene Calizo, Desalegne Teweldebrhan, Feng Miao, and Chun Ning Lau, 2008. Superior thermal conductivity of single-layer graphene. *Nano letters,* Vol. 8, Iss. 3, pp. 902-907.

[7] Rahul Raveendran Nair, Peter Blake, Alexander N Grigorenko, Konstantin S Novoselov, Tim J Booth, Tobias Stauber, Nuno MR Peres, and Andre K Geim, 2008. The fine structure constant defines the visual transparency of graphene. *Science,* Vol. 320, Iss.5881, pp. 1308-1308.

[8] Feng Wang, Yuanbo Zhang, Chuanshan Tian, Caglar Girit, Alex Zettl, Michael Crommie, and Y Ron Shen, 2008. Gate-variable optical transitions in graphene. *Science*, Vol. 320, Iss. 5873, pp. 206-209.

[9] O. Leenaerts, B. Partoens, and FM Peeters, 2008. Adsorption of H_2O, NH_3, CO, NO_2, and NO on graphene: A first-principles study. *Physical Review B*, Vol. 77, Iss. 12, pp. 125416.

[10] Jing-wen Feng, Yue-jie Liu, Hong-xia Wang, Jing-xiang Zhao, Qing-hai Cai, and Xuan-zhang Wang, 2014. Gas adsorption on silicene: a theoretical study. *Computational Materials Science*, Vol.87, pp. 218-226.

[11] Michal W Ochapski, and Michel P De Jong, 2022. Progress in epitaxial growth of stanene. *Open Physics*, Vol. 20, Iss. 1, pp. 208-223.

[12] A Dal Corso, 1996. Reciprocal Space Integration and Special-Point Techniques. *Quantum-Mechanical Ab-initio Calculation of the Properties of Crystalline Materials*, Vol. 67, pp. 77-89.

[13] Hendrik J Monkhorst and James D Pack, 1976. Special points for Brillouin-zone integrations. *Physical Review B*, Vol. 13, Iss. 12, 5188.

[14] Pere Miro, Martha Audiffred, and Thomas Heine, 2014. An atlas of two-dimensional materials. Chemical Society Reviews, Vol. 43, Iss. 18, pp. 6537-6554.

[15] A Acun, L Zhang, P Bampoulis, M Farmanbar, A van Houselt, A N Rudenko, M Lingenfelder, G Brocks, B Poelsema, M I Katsnelson, and H J W Zandvliet, 2015. Germanene: the germanium analog of graphene. *Physics Condensed Matter*, Vol. 27, Iss. 44, 443002 (11 pp).

[16] Chen-Xiao Zhao and Jin-Feng Jia, 2020. Stanene: A good platform for topological insulators and topological superconductor. *Frontiers of Physics*, Vol. 15, Iss. 5, pp. 1-15.